

Intrinsic spin currents in bulk noncentrosymmetric ferromagnets

I. Turek

*Institute of Physics of Materials, Czech Academy of Sciences,
Žitkova 22, CZ-61600 Brno, Czech Republic*

turek@ipm.cz

November 11, 2024

Abstract

Intrinsic spin currents are encountered in noncentrosymmetric crystals without any external electric fields; these currents are caused by spin-orbit interaction. In this paper, various theoretical aspects of this phenomenon in bulk ferromagnets are studied by using group theory, perturbation expansion, and calculations for model and real systems. The group-theoretical analysis of the spin-current tensor shows that the absence of space-inversion symmetry is not a sufficient condition for appearance of the intrinsic spin currents. The perturbation expansion proves that in the regime of exchange splitting dominating over spin-orbit interaction, the spin polarization of the intrinsic currents is nearly perpendicular to the direction of magnetization. First-principles calculations are carried out for NiMnSb and CoMnFeSi ferromagnetic compounds, both featured by a tetrahedral crystallographic point group. The dependence of the spin-current tensor on the direction of magnetization is approximated by a simple quadratic formula containing two constants; the relative error of this approximation is found as small as a few percent for both compounds.

1 Introduction

Spin currents generated in various materials and devices by external electric fields belong to the most important topics in spintronics [1, 2]. In this context, the well-known phenomenon is the spin Hall effect in nonmagnetic systems [3], where the spin currents transversal to the electric field are encountered. Moreover, spin-polarized longitudinal currents can be found in certain nonmagnetic solids [4]. Similarly, spin polarization of electron currents in magnetically ordered systems attracts ongoing interest as well; this involves both systems with traditional magnetic orders [5, 6, 7, 8, 9, 10] and the recently introduced altermagnets [11, 12, 13, 14, 15].

Besides the spin currents induced by applied electric fields, it was predicted two decades ago that systems lacking space-inversion symmetry (non-centrosymmetric systems) can exhibit nonzero spin currents even without an external perturbation [16]. These intrinsic spin currents arise due to spin-orbit (SO) interaction; their consequences for properties of nonmagnetic semiconductors [17] and for improved definitions of the spin-current operator [18, 19] were discussed in the literature.

The intrinsic spin currents are also relevant for noncentrosymmetric ferromagnets, especially due to their close connection to the Dzyaloshinskii-Moriya (DM) interaction [20, 21]. This interaction can lead to an instability of the ferromagnetic order resulting in a formation of noncollinear magnetic structures, such as magnetic skyrmions [22, 23]. Full details of the relation between the spin currents and the DM interaction remain yet to be clarified; nevertheless, the rough equivalence of both quantities seems to be confirmed by existing *ab initio* calculations using different approaches [20, 21, 24, 25, 26].

The present paper addresses several topics in the theory of the intrinsic spin currents in bulk noncentrosymmetric ferromagnets. The focus is on systems with the exchange splitting dominating over the strength of SO interaction. Different tools are used in the study: perturbation expansion, group theory, and computations on model as well as *ab initio* levels. Two particular Heusler-like systems are chosen for first-principles calculations, namely, NiMnSb with $C1_b$ structure [27] and CoMnFeSi with LiMgPdSn-type structure [28], both featured by the crystallographic point group $\bar{4}3m$. Special attention is paid to the dependence of the spin currents on direction of magnetization. The main aim is to get insight into the properties of intrinsic spin currents for a comparison with the known features of field-induced spin currents [8, 9, 10] and of the DM interaction [21].

2 Methods

We assume a bulk ferromagnet with perfect translational invariance, described by an effective one-electron Hamiltonian

$$H = \bar{H} + H^{\text{ex}} + H^{\text{SO}}, \quad (1)$$

where the first term \bar{H} denotes a spin-independent part containing both local (site-diagonal) and nonlocal (hopping) contributions, the second term H^{ex} denotes a spin-dependent local exchange splitting part, and the third term H^{SO} denotes a spin-dependent local SO interaction. The exchange splitting points along a fixed unit vector $\mathbf{m} = (m_x, m_y, m_z)$, which can be identified with the direction of magnetization of the ferromagnet.

The spin current is a tensor of rank two, $Q_{\kappa\lambda}$ ($\kappa, \lambda \in \{x, y, z\}$), where the first subscript κ refers to the spin polarization while the second subscript λ refers to the spatial direction of the current. Its value at zero temperature is given by

$$Q_{\kappa\lambda} = \Omega^{-1} \sum_j \langle j | \sigma_\kappa V_\lambda | j \rangle, \quad (2)$$

where Ω denotes the volume of a large finite crystal with periodic boundary conditions and the symbol j labels all eigenstates with eigenvectors $|j\rangle$ (normalized to unity in the crystal volume Ω , $\langle j | j \rangle = 1$) and eigenvalues E_j of the Hamiltonian H . The summation extends only over the occupied eigenstates with energies E_j not exceeding the Fermi energy E_F of the system. The symbol σ_κ in Eq. (2) denotes the Pauli spin matrix and the symbol V_λ denotes the velocity (current) operator, that is spin-independent, derived from the hopping part of the term \bar{H} .

Besides the complete tensor $Q_{\kappa\lambda}$, we have also studied its projection on the unit vector \mathbf{m} . This leads to a projection vector with components P_λ defined by

$$P_\lambda = \sum_\kappa m_\kappa Q_{\kappa\lambda}, \quad (3)$$

which bears information about mutual orientation of the spin polarization of the intrinsic current and the magnetization direction.

The previous expression for the spin current, Eq. (2), can be reformulated as a complex integral

$$Q_{\kappa\lambda} = \frac{1}{2\pi i \Omega} \int_C \text{Tr} \{ \sigma_\kappa V_\lambda G(\epsilon) \} d\epsilon, \quad (4)$$

where the trace (Tr) refers to the Hilbert space of the whole finite crystal, ϵ denotes a complex energy variable, the symbol $G(\epsilon) = (\epsilon - H)^{-1}$ is the

resolvent of the Hamiltonian H , and the integration path C starts and ends at the Fermi energy E_F and it contains the occupied part of the spectrum of the Hamiltonian H in its interior. The latter expression is used in an analysis of perturbation expansion, see Section 3.1.

The vanishing of the intrinsic spin currents for centrosymmetric systems reflects the fact that the spin-current operator $\sigma_\kappa V_\lambda$ changes its sign under space inversion. However, detailed information about the shape of the spin-current tensor $Q_{\kappa\lambda}$ for arbitrary nonmagnetic and magnetic crystals demands the use of group theory. This was worked out to many details for various tensor quantities in the past [6, 29, 30, 31]; in this study we applied an approach based on projection superoperators [15].

The first-principles evaluation of the spin-current tensor was carried out using the fully relativistic tight-binding linear muffin-tin orbital (TB-LMTO) method [32, 33]. This requires a modification of Eq. (4) into the form

$$Q_{\kappa\lambda} = \frac{1}{2\pi i\Omega} \int_C \text{Tr}\{\sigma_\kappa v_\lambda g(\epsilon)\} d\epsilon, \quad (5)$$

where v_λ and $g(\epsilon)$ denote respectively the effective velocity operator and the auxiliary resolvent of the TB-LMTO technique. It can be proved that Eq. (5) is invariant with respect to the screening transformations of the TB-LMTO method. Numerical implementation and computational details used were similar to those described in the previous studies of the anomalous [32] and spin [33] Hall conductivities.

3 Results and discussion

3.1 Polarization of spin currents

Let us start with an analysis of perturbation expansion of the spin-current tensor corresponding to inclusion of the term H^{SO} into the Hamiltonian $H = H_0 + H^{\text{SO}}$ with the reference nonrelativistic Hamiltonian $H_0 = \bar{H} + H^{\text{ex}}$. The resolvent $G(\epsilon)$ and the reference resolvent $G_0(\epsilon) = (\epsilon - H_0)^{-1}$ are related by

$$G(\epsilon) = G_0(\epsilon) + G_0(\epsilon)H^{\text{SO}}G_0(\epsilon) + \dots \quad (6)$$

Substitution of this relation into Eq. (4) and using the properties of nonrelativistic systems results in the well-known linear scaling of the spin-current tensor components $Q_{\kappa\lambda}$ with the strength of SO interaction, as has also been found in recent calculations for realistic systems [21].

However, the scaling of the projection vector P_λ , Eq. (3), is featured by an exponent higher than unity. This can be seen from the expansion

$P_\lambda = P_\lambda^{(0)} + P_\lambda^{(1)} + \dots$, where the individual terms correspond to those in Eq. (6). We get not only $P_\lambda^{(0)} = 0$ (needed for a linear scaling), but also $P_\lambda^{(1)} = 0$ (leading to a quadratic scaling). The latter follows from Eqs. (3), (4), and (6), which yield

$$P_\lambda^{(1)} = \frac{1}{2\pi i \Omega} \int_C F(\epsilon) d\epsilon, \quad F(\epsilon) = \text{Tr}\{(\mathbf{m} \cdot \boldsymbol{\sigma}) V_\lambda G_0(\epsilon) H^{\text{SO}} G_0(\epsilon)\}, \quad (7)$$

where we abbreviated $\boldsymbol{\sigma} = (\sigma_x, \sigma_y, \sigma_z)$ and $\mathbf{m} \cdot \boldsymbol{\sigma} = \sum_\kappa m_\kappa \sigma_\kappa$. Subsequently, one obtains

$$F(\epsilon) = \text{Tr}\{G_0(\epsilon) V_\lambda G_0(\epsilon) H^{\text{SO}}(\mathbf{m} \cdot \boldsymbol{\sigma})\} = 0. \quad (8)$$

In the first step, we used the cyclic invariance of the trace together with the fact that the operator $\mathbf{m} \cdot \boldsymbol{\sigma}$ commutes with the reference Hamiltonian H_0 and with its resolvent $G_0(\epsilon)$. In the second step, we used the facts that the operator $H^{\text{SO}}(\mathbf{m} \cdot \boldsymbol{\sigma})$ is site-diagonal and that the on-site blocks of the operator $G_0(\epsilon) V_\lambda G_0(\epsilon)$ vanish, see Eq. (23) in Ref. [32]. This proves Eq. (8) and, consequently, the vanishing of $P_\lambda^{(1)}$.

This conclusion is supported by calculations for a tight-binding model of a one-dimensional chain along the x axis, described in detail in Appendix A. In this model, the values of index λ are confined to $\lambda = x$ and the remaining components of the spin-current tensor and of the projection vector are displayed in Fig. 1 as functions of the strength of SO interaction. One can see clearly the linear scaling of the tensor components Q_{xx} , Q_{yx} , and Q_{zx} , in contrast to the quadratic scaling of the only component P_x of the projection vector.

This result means that in the regime of exchange splitting dominating over SO interaction, the spin polarization of the intrinsic spin currents is practically perpendicular to the magnetization direction. This feature contrasts the properties of field-induced spin currents in collinear nonrelativistic magnets, where the spin polarization of the current is always strictly parallel to the direction of magnetic moments, both in ferromagnets and altermagnets [10, 15]. In ferromagnets with nonzero SO interaction, the spin polarization of the transversal currents (spin Hall effect) also contains a nonnegligible component parallel to the magnetization direction [8, 9].

3.2 Group-theoretical analysis

For crystals without spontaneous magnetic order, the shape of the spin-current tensor $Q_{\kappa\lambda}$ is dictated by the crystallographic point group. This tensor vanishes for all centrosymmetric point groups; for all noncentrosymmetric point groups, the numbers of independent components of the tensor

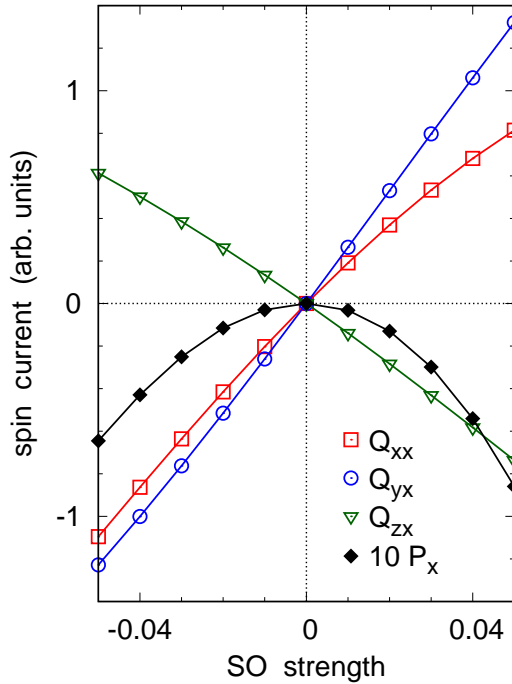


Figure 1: Spin currents in the one-dimensional model as functions of the strength of SO interaction: components of the spin-current tensor $Q_{\kappa x}$ (open symbols) and of the projection vector P_x (full diamonds, magnified by a factor of ten).

are listed in Table 1. One can see that symmetry reduction of the system leads in general to an increase of the number of independent components, as expected. However, one also finds that three particular groups ($\bar{6}$, $\bar{6}m2$, $\bar{4}3m$) yield vanishing spin-current tensors, despite the absence of space inversion. Note that these three groups form a special class from the viewpoint of chiral structures and related physical properties [34].

For magnetically ordered crystals, one has to use the magnetic point groups. Among the total number of 122 magnetic point groups, only 21 groups are noncentrosymmetric and compatible with ferromagnetic order. For all these groups, the numbers of independent components of the spin-current tensor are listed in Table 2. One can see that most of these groups support the existence of nonzero spin currents; the only exceptions are two hexagonal groups ($\bar{6}$, $\bar{6}m'2'$). Note that both groups also lead to vanishing SO torques generated by external electric fields [35].

One can thus observe that both in nonmagnetic and ferromagnetic crys-

Table 1: Numbers of independent components of the spin-current tensor for all noncentrosymmetric crystallographic point groups of nonmagnetic solids.

point group	no. of components
1	9
2	5
m	4
222, 3, 4, 6	3
$2mm$, 32, 422, $\bar{4}$, 622	2
$3m$, $4mm$, $\bar{4}2m$, $6mm$, 23, 432	1
$\bar{6}$, $\bar{6}m2$, $\bar{4}3m$	0

Table 2: Numbers of independent components of the spin-current tensor for all noncentrosymmetric magnetic point groups compatible with ferromagnetism.

magnetic point group	no. of components
1	9
2, 2'	5
m , m'	4
3, 4, 6, 2'2'2	3
$\bar{4}$, $m'm'2$, $m'm'2'$, 32', 42'2', 62'2'	2
$3m'$, $4m'm'$, $\bar{4}2'm'$, $6m'm'$	1
$\bar{6}$, $\bar{6}m'2'$	0

Table 3: Independent components $Q_{\kappa\lambda}$ of the spin-current tensor in NiMnSb and CoMnFeSi alloys for magnetization parallel to three high-symmetry directions. The values obtained from the least-squares fit are displayed in parenthesis.

magnetization direction	indices $\kappa\lambda$	$Q_{\kappa\lambda}$ (meV/nm ²) NiMnSb	$Q_{\kappa\lambda}$ (meV/nm ²) CoMnFeSi
(001)	yy	-0.546(-0.537)	1.202(1.210)
(111)	xy	-0.179(-0.185)	0.409(0.404)
(101)	zz	-0.261(-0.268)	0.615(0.605)
(101)	zx	-0.280(-0.277)	0.600(0.606)

tals, missing space-inversion symmetry does not represent a sufficient condition for the presence of nonzero intrinsic spin currents.

3.3 Spin currents in NiMnSb and CoMnFeSi alloys

The real systems selected for *ab initio* study are NiMnSb with $C1_b$ structure [27] and CoMnFeSi with LiMgPdSn-type structure [28], both belonging to the crystallographic space group $F\bar{4}3m$ (No. 216). Their structures (related closely to the standard Heusler structure) are derived from an fcc Bravais lattice with four sublattices, labelled A , B , C , and D , which are shifted mutually along the (111) direction of the cubic lattice. The basis vectors of these sublattices are: $A(0, 0, 0)$, $B(0.25, 0.25, 0.25)$, $C(0.5, 0.5, 0.5)$, and $D(0.75, 0.75, 0.75)$, all in units of the fcc lattice parameter. The sublattice occupation in both compounds is: Ni(A)Mn(B)Sb(D) (with C sublattice empty) and Co(A)Mn(B)Fe(C)Si(D). Their total magnetic moment is around $4 \mu_B$ per formula unit [27, 28], indicating that both systems are in a regime of strong exchange splitting.

The crystallographic point group of these systems (with ferromagnetic order ignored) is $\bar{4}3m$, which belongs to the three special noncentrosymmetric groups leading to vanishing spin currents, see Table 1. This means that nonzero spin currents appearing in the ferromagnetic state have to be ascribed solely to the magnetic order. The calculated spin-current tensor for the magnetization direction \mathbf{m} along three high-symmetry directions of the lattice is shown in Table 3. For $\mathbf{m}||$ (001), the magnetic point group is $\bar{4}2'm'$ and the only independent nonzero tensor component is $Q_{xx} = -Q_{yy}$. For $\mathbf{m}||$ (111), the group is $3m'$ and the only component is $Q_{xy} = Q_{yz} = Q_{zx} = -Q_{yx} = -Q_{zy} = -Q_{xz}$. For $\mathbf{m}||$ (101), the group is $m'm'2'$ leading to two

slightly different components, namely, $Q_{xx} = -Q_{zz}$ and $Q_{xz} = -Q_{zx}$.

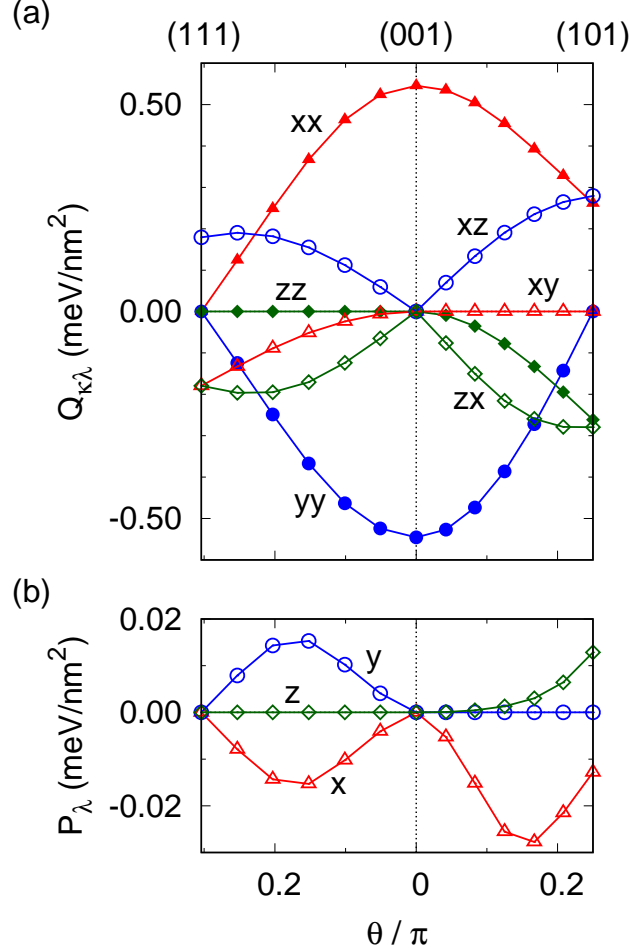


Figure 2: Calculated spin currents in NiMnSb for magnetization direction varying along the path (111) – (001) – (101): components of the spin-current tensor $Q_{\kappa\lambda}$ (a) and of the projection vector P_λ (b). For the missing components $Q_{\kappa\lambda}$, see text.

More complete information about the spin currents can be obtained by inspecting the spin current tensor $Q_{\kappa\lambda}$ and the projection vector P_λ for magnetization direction \mathbf{m} varying along the path (111) – (001) – (101). In terms of spherical angles θ and ϕ , it holds $m_x = \sin \theta \cos \phi$, $m_y = \sin \theta \sin \phi$, $m_z = \cos \theta$, and the segment (111) – (001) is featured by $\phi = \pi/4$, while the segment (001) – (101) is featured by $\phi = 0$.

The resulting dependences are displayed in Fig. 2 and Fig. 3 for NiMnSb and CoMnFeSi, respectively. The magnetic point group inside the segment

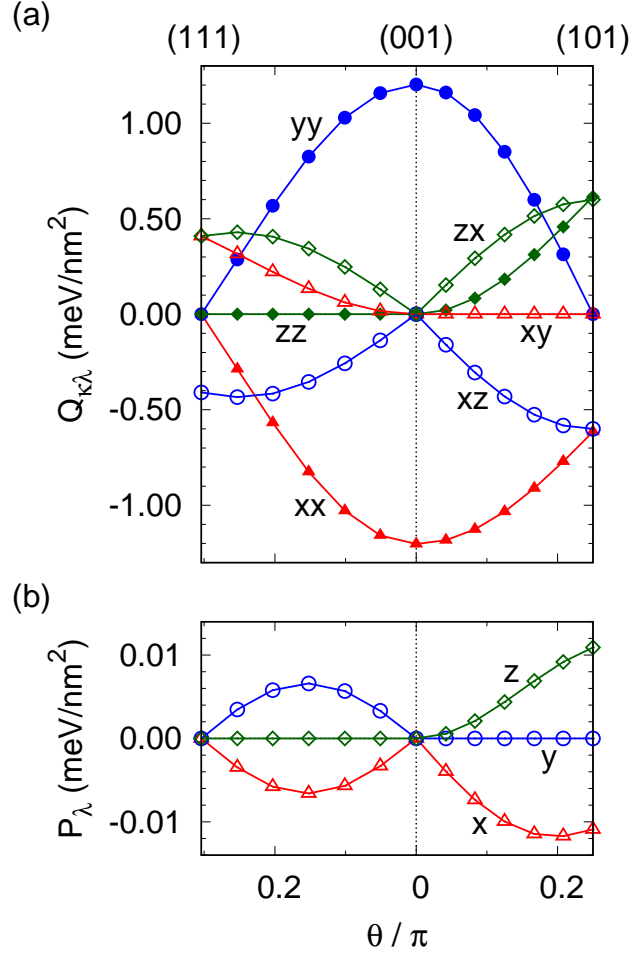


Figure 3: The same as Fig. 2, but for CoMnFeSi.

(111) – (001) is m' and the spin-current tensor has four independent nonzero components ($Q_{xx} = -Q_{yy}$, $Q_{xy} = -Q_{yx}$, $Q_{xz} = -Q_{yz}$, $Q_{zx} = -Q_{zy}$). The magnetic point group inside the segment (001) – (101) is $2'$ leading to five components (Q_{xx} , Q_{yy} , Q_{zz} , Q_{xz} , Q_{zx}). All numerical results are consistent with the tensor shapes obtained from the group theory (Section 3.2).

It can also be seen that magnitudes of all components of the projection vector P_λ are substantially smaller than the range of the spin-current values $Q_{\kappa\lambda}$. This agrees fully with conclusions of Section 3.1 about an approximate orthogonality between the spin polarization of the intrinsic currents and the direction of magnetization.

3.4 Dependence on magnetization direction

Undoubtedly, deep understanding to the spin currents in ferromagnets calls for an assessment of the dependence of the tensor $Q_{\kappa\lambda}$ on the magnetization direction \mathbf{m} . Since the spin-current operator $\sigma_\kappa V_\lambda$ does not change sign due to time reversal, this dependence has to satisfy exactly the rule $Q_{\kappa\lambda}(-\mathbf{m}) = Q_{\kappa\lambda}(\mathbf{m})$. An approximate form of this dependence can be derived under several assumptions. We assume, e.g., that the Fermi energy of the system and the magnitude of the exchange splitting in the Hamiltonian H , Eq. (1), do not change with varying \mathbf{m} . If we confine ourselves to the simplest dependence compatible with the mentioned rule, we have to consider a quadratic law

$$\tilde{Q}_{\kappa\lambda}(\mathbf{m}) = \sum_{\mu\nu} T_{\kappa\lambda\mu\nu} m_\mu m_\nu, \quad (9)$$

where the $T_{\kappa\lambda\mu\nu}$ are components of a tensor of rank four. This tensor is symmetric in the indices μ and ν ($T_{\kappa\lambda\mu\nu} = T_{\kappa\lambda\nu\mu}$) and it has to be invariant with respect to all elements of the crystallographic point group of the underlying nonmagnetic system. This yields conditions

$$T_{\kappa\lambda\mu\nu} = |\alpha| \sum_{\kappa'\lambda'\mu'\nu'} \alpha_{\kappa\kappa'} \alpha_{\lambda\lambda'} \alpha_{\mu\mu'} \alpha_{\nu\nu'} T_{\kappa'\lambda'\mu'\nu'}, \quad (10)$$

where $\{\alpha_{\mu\nu}\}$ are real orthogonal 3×3 matrices representing the elements α of the point group and $|\alpha|$ denotes determinant of α . These conditions and the symmetry property define the shape of the tensor $T_{\kappa\lambda\mu\nu}$. The numbers of independent components of this tensor for all noncentrosymmetric point groups are listed in Table 4.

One can find that in the case of the point group $\bar{4}3m$ (full symmetry group of a regular tetrahedron), there are only two independent components of the tensor $T_{\kappa\lambda\mu\nu}$; the corresponding dependence, Eq. (9), reduces to

$$\begin{aligned} \tilde{Q}_{xx} &= A(m_y^2 - m_z^2), \\ \tilde{Q}_{yy} &= A(m_z^2 - m_x^2), \\ \tilde{Q}_{zz} &= A(m_x^2 - m_y^2), \\ \tilde{Q}_{xy} &= -\tilde{Q}_{yx} = A' m_x m_y, \\ \tilde{Q}_{yz} &= -\tilde{Q}_{zy} = A' m_y m_z, \\ \tilde{Q}_{zx} &= -\tilde{Q}_{xz} = A' m_x m_z, \end{aligned} \quad (11)$$

where A and A' are two constants. Note that the constants A and A' define separately the diagonal and nondiagonal components of the tensor $\tilde{Q}_{\kappa\lambda}$.

In order to check the validity of the approximate dependence, Eq. (11), calculations for a number of unit vectors \mathbf{m} were carried out and the resulting

Table 4: Numbers of independent components of the tensor $T_{\kappa\lambda\mu\nu}$ for all noncentrosymmetric crystallographic point groups.

point group	no. of components
1	54
2	28
m	26
3	18
222	15
4, $\bar{4}$	14
$2mm$	13
6	12
32	10
$3m, 422$	8
$\bar{4}2m, 622$	7
$4mm, \bar{6}$	6
$6mm, 23$	5
$\bar{6}m2, 432$	3
$\bar{4}3m$	2

values of $Q_{\kappa\lambda}(\mathbf{m})$ were compared to the values of $\tilde{Q}_{\kappa\lambda}(\mathbf{m})$ with the constants A and A' obtained from a least-squares fit. The sampling vectors \mathbf{m} are shown in Fig. 4; they were chosen to scan the region among the three high-symmetry directions of the system.

The resulting constants are: $A = -0.537$ meV/nm² and $A' = -0.554$ meV/nm² for NiMnSb while $A = 1.210$ meV/nm² and $A' = 1.212$ meV/nm² for CoMnFeSi. One can see that $A \approx A'$ for both systems. It can also be observed that for $A = A'$, the approximate dependence, Eq. (11), satisfies a sum rule $\sum_{\kappa} m_{\kappa} \tilde{Q}_{\kappa\lambda}(\mathbf{m}) = 0$ for all λ and \mathbf{m} , so that the magnetization direction is exactly orthogonal to the spin polarization of the approximate spin currents. In other words, the small relative difference between A and A' reflects the small values of the projection vector P_{λ} (Section 3.3).

The accuracy of the developed scheme can be quantified, e.g., by comparing the calculated and fitted spin currents for the high-symmetry directions, which indicates a very good agreement, see Table 3. A more systematic comparison should include all sampling vectors \mathbf{m} used for the fit (Fig. 4). A relative deviation can be defined as the maximum over all κ , λ , and \mathbf{m} of the quantity $|Q_{\kappa\lambda}(\mathbf{m}) - \tilde{Q}_{\kappa\lambda}(\mathbf{m})|/|A|$. This deviation comes out 0.037 for NiMnSb and 0.0094 for CoMnFeSi, so that it does not exceed a few percent

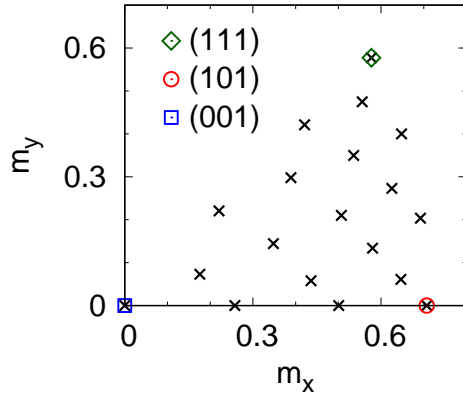


Figure 4: Projection of the sampling directions \mathbf{m} on the $x - y$ plane.

in the studied systems. This analysis proves that the derived quadratic formula with two constants, Eq. (11), provides a good starting point for more accurate approximations of the full dependence of the spin-current tensor on magnetization direction.

4 Conclusions

This pilot theoretical study has been devoted to spin currents which are not induced by external electric fields but arise only due to spin-orbit interaction in the absence of space-inversion symmetry. The group analysis revealed that these spin currents appear nearly in all bulk systems with noncentrosymmetric magnetic point groups compatible with ferromagnetism; the only exceptions are systems with point groups $\bar{6}$ and $\bar{6}m'2'$, where the symmetry also leads to vanishing spin-orbit torques due to external electric fields.

The study has focused on systems with weak spin-orbit interaction as compared to exchange splitting. In this regime, the analysis of a perturbation expansion proved that spin polarization of the intrinsic currents is nearly perpendicular to the direction of magnetization. This property differs from that of currents generated by external electric fields, where the spin polarization of the current contains a substantial component parallel to the magnetization.

The general conclusions drawn have been corroborated by *ab initio* calculations for NiMnSb and CoMnFeSi compounds, for which the dependence of the spin-current tensor on the magnetization direction has also been studied. A simple quadratic approximation of this dependence has been derived and its accuracy checked; relative deviations not exceeding a few percent

have been found for both systems. In view of the close relation between the intrinsic spin currents and the Dzyaloshinskii-Moriya interaction, one can expect that results of similar studies for other ferromagnets will serve as an input for micromagnetic simulations of systems that are collinear on a short length scale, but noncollinear on a longer scale, such as spin spirals, magnetic domain walls, and skyrmions.

Acknowledgments

This work was supported financially by the Czech Science Foundation (grant No. 23-04746S). The author thanks Dr. Karel Carva and Dr. Alberto Marmodoro for stimulating discussions.

A One-dimensional tight-binding model

The structure of the one-dimensional model is depicted in Fig. 5: an infinite periodic chain along the x axis comprising one magnetic site and one nonmagnetic site in the unit cell, with all sites lying in the $x - y$ plane.

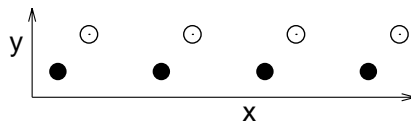


Figure 5: Structure of the one-dimensional chain with magnetic (full circles) and nonmagnetic (open circles) sites.

The tight-binding Hamiltonian assumes three p -type orbitals attached to each magnetic site and one s -type orbital attached to each nonmagnetic site. The exchange splitting at each magnetic site has a form $\mathbf{b} \cdot \boldsymbol{\sigma}$, where $\mathbf{b} = (b_x, b_y, b_z)$ is the exchange field, while SO interaction at the same site has a form $\xi \mathbf{L} \cdot \boldsymbol{\sigma}$, where $\mathbf{L} = (L_x, L_y, L_z)$ is the operator of orbital momentum and ξ denotes the strength of SO interaction. Nonzero hopping integrals are assumed between: (i) the p orbitals of the nearest-neighbor magnetic sites, (ii) each s orbital and its two nearest p_x orbitals, and (iii) each s orbital and its first nearest p_y orbital. After a downfolding of the s orbitals, an effective Hamiltonian for the magnetic sites with p orbitals is obtained. Its lattice Fourier transformation can be represented by a matrix $H_{\mu s, \mu' s'}(k)$, where k is the one-dimensional reciprocal-space variable, $\mu, \mu' \in \{x, y, z\}$ refer to the particular p orbital, and $s, s' \in \{\uparrow, \downarrow\}$ are the spin indices.

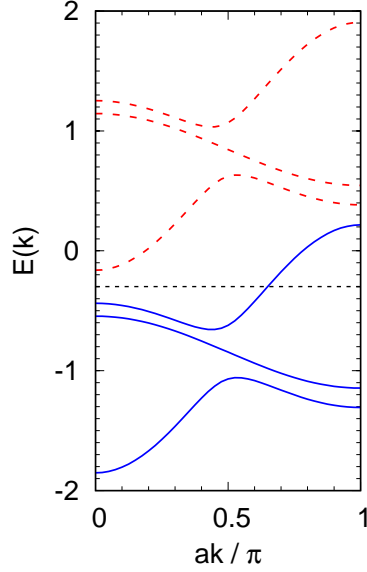


Figure 6: Bandstructure of the one-dimensional model with null SO interaction ($\xi = 0$): majority bands (full lines) and minority bands (dashed lines). The horizontal short-dashed line denotes the position of the Fermi level E_F .

The resulting Hamiltonian has a form of Eq. (1), where both local terms lead to k -independent matrices

$$H_{\mu s, \mu' s'}^{\text{ex}} = \delta_{\mu \mu'} \sum_{\lambda} b_{\lambda} (\sigma_{\lambda})_{ss'} \quad (12)$$

and

$$H_{\mu s, \mu' s'}^{\text{SO}} = \xi \sum_{\lambda} (L_{\lambda})_{\mu \mu'} (\sigma_{\lambda})_{ss'}, \quad (13)$$

where we set $(L_{\lambda})_{\mu \mu'} = -i \varepsilon_{\mu \mu' \lambda}$ with $\varepsilon_{\mu \mu' \lambda}$ denoting the Levi-Civita tensor. The spin-independent term \bar{H} becomes a k -dependent matrix,

$$\begin{aligned} \bar{H}_{\mu s, \mu' s'}(k) &= \delta_{ss'} W_{\mu \mu'}(k), \\ W_{xx}(k) &= -2h_{xx} \cos(ak), \\ W_{yy}(k) &= 2h_{yy} \cos(ak), \\ W_{zz}(k) &= 2h_{zz} \cos(ak), \\ W_{yx}(k) &= h_n - h'_n \exp(iak), \\ W_{zx}(k) &= W_{yz}(k) = 0, \end{aligned} \quad (14)$$

where all omitted matrix elements can be restored from $W_{\mu' \mu}(k) = W_{\mu \mu'}^*(k)$. Here a is the lattice parameter and h_{xx} , h_{yy} , h_{zz} , h_n , and h'_n are hopping

parameters of the model. The representation of the velocity operator V_x is obtained from the relation $(V_x)_{\mu s, \mu' s'}(k) = \delta_{ss'} dW_{\mu\mu'}(k)/dk$.

The calculations were carried out with following values of the model parameters: $b_x = 0.195$, $b_y = 0.26$, $b_z = 0.78$, $h_{xx} = 0.5$, $h_{yy} = 0.2$, $h_{zz} = 0.15$, $h_n = 0.2$, and $h'_n = 0.1$, and with the Fermi energy $E_F = -0.3$; the band-structure of the model for $\xi = 0$ is shown in Fig. 6. For evaluation of the spin currents, Eq. (2), a Lorentzian broadening of the eigenvalues with a parameter $\gamma = 0.01$ was used and the strength of SO interaction was varied in the interval $-0.05 \leq \xi \leq 0.05$, see Fig. 1.

References

- [1] E. Y. Tsymbal and I. Žutić, editors. *Handbook of Spin Transport and Magnetism*. CRC Press, Boca Raton, 2012.
- [2] S. Maekawa, S. O. Valenzuela, E. Saitoh, and T. Kimura, editors. *Spin Current*. Oxford University Press, 2012.
- [3] J. Sinova, S. O. Valenzuela, J. Wunderlich, C. H. Back, and T. Jungwirth. *Rev. Mod. Phys.*, 87:1213, 2015.
- [4] S. Wimmer, M. Seemann, K. Chadova, D. Ködderitzsch, and H. Ebert. *Phys. Rev. B*, 92:041101(R), 2015.
- [5] B. Zimmermann, K. Chadova, D. Ködderitzsch, S. Blügel, H. Ebert, D. V. Fedorov, N. H. Long, P. Mavropoulos, I. Mertig, Y. Mokrousov, and M. Gradhand. *Phys. Rev. B*, 90:220403(R), 2014.
- [6] M. Seemann, D. Ködderitzsch, S. Wimmer, and H. Ebert. *Phys. Rev. B*, 92:155138, 2015.
- [7] Y. Zhang, Y. Sun, H. Yang, J. Železný, S. P. P. Parkin, C. Felser, and B. Yan. *Phys. Rev. B*, 95:075128, 2017.
- [8] V. P. Amin, J. Li, M. D. Stiles, and P. M. Haney. *Phys. Rev. B*, 99:220405(R), 2019.
- [9] N. Soya, M. Yamada, K. Hamaya, and K. Ando. *Phys. Rev. Lett.*, 131:076702, 2023.
- [10] K. D. Belashchenko. *Phys. Rev. B*, 109:054409, 2024.
- [11] R. González-Hernández, L. Šmejkal, K. Výborný, Y. Yahagi, J. Sinova, T. Jungwirth, and J. Železný. *Phys. Rev. Lett.*, 126:127701, 2021.

- [12] D.-F. Shao, S.-H. Zhang, M. Li, C.-B. Eom, and E. Y. Tsymbal. *Nat. Commun.*, 12:7061, 2021.
- [13] L. Šmejkal, A. B. Hellenes, R. González-Hernández, J. Sinova, and T. Jungwirth. *Phys. Rev. X*, 12:011028, 2022.
- [14] L. Šmejkal, J. Sinova, and T. Jungwirth. *Phys. Rev. X*, 12:040501, 2022.
- [15] I. Turek. *Phys. Rev. B*, 106:094432, 2022.
- [16] E. I. Rashba. *Phys. Rev. B*, 68:241315(R), 2003.
- [17] E. I. Rashba. *Phys. Rev. B*, 70:161201(R), 2004.
- [18] Y. Wang, K. Xia, Z.-B. Su, and Z. Ma. *Phys. Rev. Lett.*, 96:066601, 2006.
- [19] J. Shi, P. Zhang, D. Xiao, and Q. Niu. *Phys. Rev. Lett.*, 96:076604, 2006.
- [20] T. Kikuchi, T. Koretsune, R. Arita, and G. Tatara. *Phys. Rev. Lett.*, 116:247201, 2016.
- [21] F. Freimuth, S. Blügel, and Y. Mokrousov. *Phys. Rev. B*, 96:054403, 2017.
- [22] S. Seki and M. Mochizuki. *Skyrmions in Magnetic Materials*. Springer, Cham, 2016.
- [23] J. H. Han. *Skyrmions in Condensed Matter*. Springer, Cham, 2017.
- [24] F. Freimuth, S. Blügel, and Y. Mokrousov. *J. Phys.: Condens. Matter*, 26:104202, 2014.
- [25] S. Mankovsky and H. Ebert. *Phys. Rev. B*, 96:104416, 2017.
- [26] S. Mankovsky, S. Polesya, and H. Ebert. *Phys. Rev. B*, 99:104427, 2019.
- [27] I. Galanakis, P. H. Dederichs, and N. Papanikolaou. *Phys. Rev. B*, 66:134428, 2002.
- [28] L. Bainsla, A. I. Mallick, M. M. Raja, A. K. Nigam, B. S. D. Ch. S. Varaprasad, Y. K. Takahashi, A. Alam, K. G. Suresh, and K. Hono. *Phys. Rev. B*, 91:104408, 2015.
- [29] R. R. Birss. *Rep. Prog. Phys.*, 26:307, 1963.

- [30] W. H. Kleiner. *Phys. Rev.*, 142:318, 1966.
- [31] S. V. Gallego, J. Etxebarria, L. Elcoro, E. S. Tasci, and J. M. Perez-Mato. *Acta Cryst. A*, 75:438, 2019.
- [32] I. Turek, J. Kudrnovský, and V. Drchal. *Phys. Rev. B*, 89:064405, 2014.
- [33] I. Turek, J. Kudrnovský, and V. Drchal. *Phys. Rev. B*, 100:134435, 2019.
- [34] G. H. Fecher, J. Kübler, and C. Felser. *Materials*, 15:5812, 2022.
- [35] S. Wimmer, K. Chadova, M. Seemann, D. Ködderitzsch, and H. Ebert. *Phys. Rev. B*, 94:054415, 2016.